A multiband sub-6 THz patch antenna with high gain for IoT and 6G communication

Redwan Al Mahmud Bin Asad Ananta[1], Md. Sharif Ahammed[1], Md. Ashraful Haque[1], Narinderjit Singh Sawaran Singh[2], Kamal Hossain Nahin[1], Jamal Hossain Nirob[1], Md. Kawsar Ahmed[1], Liton Chandra Paul[3]

[1]Department of Electrical and Electronic Engineering, Daffodil International University, Dhaka, Bangladesh
[2]Faculty of Data Science and Information Technology, INTI International University, Nilai, Malaysia
[3]Department of Electrical, Electronic and Communication Engineering, Pabna University of Science and Technology, Pabna, Bangladesh

Article Info

Article history:

Received Aug 6, 2024
Revised Mar 3, 2025
Accepted Mar 11, 2025

Keywords:

6G communication
Industrial and innovation
Microstrip patch antenna
Multiple-input multiple-output antenna
Resistor, inductor, and capacitor
Sub-6

ABSTRACT

This comprehensive study introduces a meticulously designed and characterized terahertz (THz) multiple-input multiple-output (MIMO) antenna engineered to operate within the 0.4 THz to 1.6 THz frequency range. The antenna's construction includes a copper patch and ground plane integrated into a polyimide substrate, ensuring exceptional durability and robust performance. Significantly, the antenna reveals four distinct resonance frequencies at 0.46 THz, 0.9 THz, 1.31 THz, and 1.44 THz each accompanied by bandwidths of 0.005 THz, 0.17 THz, and 0.34 THz, respectively. Moreover, the antenna delivers notable gains of 8.52 dB, 11.54 dB, and 13.25 dB at these frequencies, coupled with substantial efficiencies of 88.32%, 92.02%, and 89.89%, respectively. Additionally, the antenna showcases exceptional isolation of 26 dB, a low envelope correlation coefficient (ECC) of 0.003, and a diversity gain (DG) of 9.98. These remarkable attributes underscore the antenna's aptness for high-performance THz applications, offering substantial advantages in terms of gain, efficiency, and isolation for next-generation wireless communication systems.

Corresponding Author:

Narinderjit Singh Sawaran Singh
Faculty of Data Science and Information Technology, INTI International University
BBN, Putra Nilai, Nilai 71800, Negeri Sembilan, Malaysia
Email: narinderjits.sawaran@newinti.edu.my

1. INTRODUCTION

The rapid progress of wireless communication technologies has spurred the exploration of higher frequency bands, particularly in the terahertz (THz) range, which spans from 0.1 THz to 10 THz [1]. This frequency band is highly promising for enabling high-capacity data transmission and ultra-fast wireless communication systems, positioning it as a key focus for the development of next-generation communication networks [2]. The THz spectrum is distinguished by its ability to offer expansive bandwidths and high data rates, which are essential for a wide range of applications such as high-resolution imaging, advanced spectroscopy, and secure communications, paving the way for significant advancements in technology and communication capabilities [3].

The integration of multiple-input multiple-output (MIMO) technology into THz communication systems represents a pivotal advancement in wireless communications [4]. MIMO systems leverage multiple antennas at both the transmitter and receiver to enhance channel capacity, improve data rates, and ensure robust signal quality, making them indispensable for high-frequency applications like those in the THz spectrum. The unique challenges of the THz range, including high path losses and susceptibility to atmospheric absorption, can be effectively mitigated by MIMO antennas through spatial diversity and beamforming techniques [5]. In the sub-6 THz range, MIMO antennas enable efficient utilization of the available bandwidth while ensuring reliable communication over short to medium distances, as required by many IoT and 6G applications. Moreover, the ability of MIMO systems to minimize mutual coupling and interference between antenna elements further enhances their suitability for high-density networks [6]. Designing MIMO antennas for THz frequencies, however, demands careful consideration of isolation, gain, efficiency, and compactness to meet the stringent requirements of next-generation communication systems. By incorporating advanced materials and innovative structural designs, MIMO antennas in the THz spectrum can overcome these challenges, offering exceptional performance in terms of bandwidth, signal strength, and diversity gain, thus unlocking new possibilities for ultrafast and high-capacity wireless networks [7].

The designed antenna exhibits three distinct resonance frequencies at 0.46 THz, 0.9 THz, and 1.31 THz, with corresponding bandwidths of 0.005 THz, 0.17 THz, and 0.34 THz, respectively. These features mark a significant improvement over the bandwidths reported in Table 1, where references [1]-[4], [6] exhibit bandwidths of 0.3 THz, 0.6 THz, and 0.4 THz. The superior bandwidth, particularly at higher frequencies, allows for more efficient data transmission and greater channel capacity, making this antenna highly suitable for high-speed communication systems. Additionally, the antenna achieves notable gains of 8.52 dB, 11.54 dB, and 13.25 dB at the respective resonance frequencies, significantly surpassing the gains reported in Table 1, which range from 4-10 dB. The high gain values indicate stronger signal reception and transmission capabilities, enhancing the overall performance of the communication system. Furthermore, the antenna demonstrates efficiencies of 88.32%, 92.02%, and 89.89% across the three frequencies, ensuring minimal energy loss and maximal signal strength.

The antenna also excels in isolation, with an impressive value of 26 dB, indicating excellent separation between the antenna elements. This high level of isolation reduces mutual coupling and interference, crucial for maintaining the integrity of transmitted and received signals in MIMO systems. Moreover, the low envelope correlation coefficient (ECC) of 0.003 and high diversity gain (DG) of 9.98 underscore the antenna's suitability for MIMO applications. The low ECC value indicates minimal signal correlation, leading to better signal diversity and reduced fading effects, while the high DG ensures robust performance in multipath environments. In conclusion, the combination of broad frequency range, high gain, exceptional efficiency, superior isolation, and high diversity gain makes this antenna an outstanding candidate for high-performance wireless communication systems, particularly in MIMO applications where superior signal quality, minimal interference, and efficient energy use are paramount.

Table 1. Performance comparisons with the published state of the art

Reference	BW (THz)	Antenna size (μm^2)	Isolation (dB)	Gain (dB)	Efficiency (%)	ECC DG (dB)	Substrate material
[8]	0.3	120×90	-54	$4.5 - 10$	NA	0.000023/ 9.99	NA
[9]	0.6	130×85	-55	7.23	NA	0.000168/ 9.999	NA
[10]	0.11	NA	-25	4.45	N/A	0.0372/ 9.99	Silicon dioxide
[11]	1	70×35	-23	NA	98	0.004859/ 9.99	Teflon
[12]	NA	$380\times$ 380	-20	8.28	NA	NA	Pyrex
[13]	0.4	600×300	-25	5.49	85.24	0.015/9.99	Polyimide
This work	0.005, 0.17, 0.34	65×180	-26	8.52, 11.54, 13.25	88.32, 92.02, 89.89	0.003/9.98	Polyimide

– Single-element antenna

Figure 1 shows the detailed architecture of the single-element antenna. Both the ground and radiator or patch are made of copper. The patch has a length of 150 μm, a width of 200 μm, and a thickness of 0.5

µm. The patch is etched on a Polyimide substrate having a dielectric constant of 3.5, a height of 30 µm, and a total size of 270×280 µm^2. The patch is fed by a 50 Ω microstrip line having a dimension of 110×25 µm^2. Two insets are created to match the impedance having a dimension of 30×5 µm^2. To enhance the antenna performance, some slots are created based on the surface current distribution of the antenna. Initially, a vertical I-shaped slot is introduced on both sides of the patch, having a dimension of 100×10 µm^2. Again, another vertical I-shaped slot and two adjacent rectangular slots are etched on top of the patch, having a dimension of 15×70 µm^2 and 30×15 µm^2 respectively. Finally, based on surface current, a flower-shaped slot is created at the center of the patch. This flower shape consists of a circle at the center and four circles surrounding it, each having a radius of 15 µm.

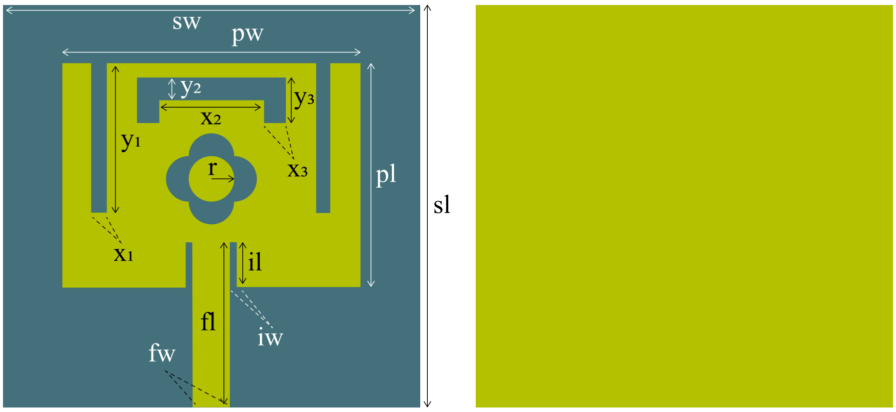

(i) Front (ii) Back

Figure 1. Schematic of the single element-antenna

Here, sw=280 µm; sl=270 µm; pw=200 µm; pl=150 µm; fw=25 µm; fl=110 µm; iw= 5 µm; il= 30 µm; x1=10 µm; y1=100 µm; x2=70 µm; y2=15 µm; x3=15 µm; y3=30 µm; and r=15 µm.

– Multiple-input multiple-output antenna

To enhance the system's reliability, a 1×2 MIMO antenna is proposed, depicted in Figure 2. One antenna element is 180° rotated and placed upside-down position with another. The antenna elements are 140 µm apart from each other. The substrate dimension of the MIMO antenna is 600×280 µm^2.

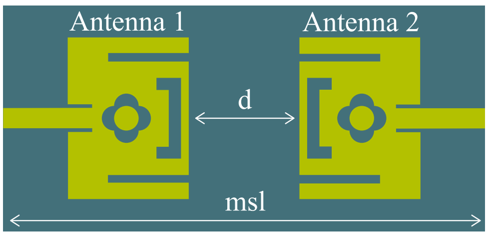

Figure 2. Schematic of the 1×2 MIMO antenna

Here, msl=600 µm and d=150 µm.

2. RESULT AND DISCUSSION

2.1. Single-element antenna

The reflection coefficient, denoted as S11, quantifies the amount of power reflected by the antenna upon transmitting a signal. The statement denotes the effectiveness of achieving impedance matching between the antenna and the transmission line [8]. The single-element microstrip patch antenna's simulated reflection coefficient (S11) showed three distinct resonance frequencies at 0.4624 THz, 0.912 THz, and 1.448 THz, shown in Figure 3(a). The antenna showed negligible reflection at these frequencies, indicating effective impedance matching. The resonances have bandwidths of 0.04 THz, 0.16 THz, and 0.33 THz, covering frequency ranges of 0.44-0.48 THz, 0.81-0.97 THz, and 1.23-1.56 THz and return loss of -22 dB, -49 dB, and -47 dB, respectively. The bandwidths refer to the frequency ranges where the reflection coefficient stays below -10 dB, indicating efficient radiation and impedance matching. The antenna's capacity to efficiently function across a wide variety of THz frequencies is demonstrated by its many resonance frequencies and significant bandwidths [14]. This makes it appropriate for various applications within the THz spectrum.

The single-element antenna demonstrates remarkable performance in terms of both gain and efficiency across its three operating frequency ranges, as shown in Figure 3(b). The antenna attains a maximum gain of 8.9 dB, 11.81 dB, and 12.23 dB, respectively. The gain represents the antenna's capacity to efficiently focus radiated power, with higher gains indicating superior directional performance [15].

The antenna exhibits exceptional efficiency over its entire range of operational frequencies. The efficiency at the resonance frequencies is 86%, 92%, and 90%, respectively. The efficiency figures indicate the proportion of power that the antenna effectively radiates relative to the power input, with minimum losses. This suggests that the antenna effectively converts input power into radiated electromagnetic waves.

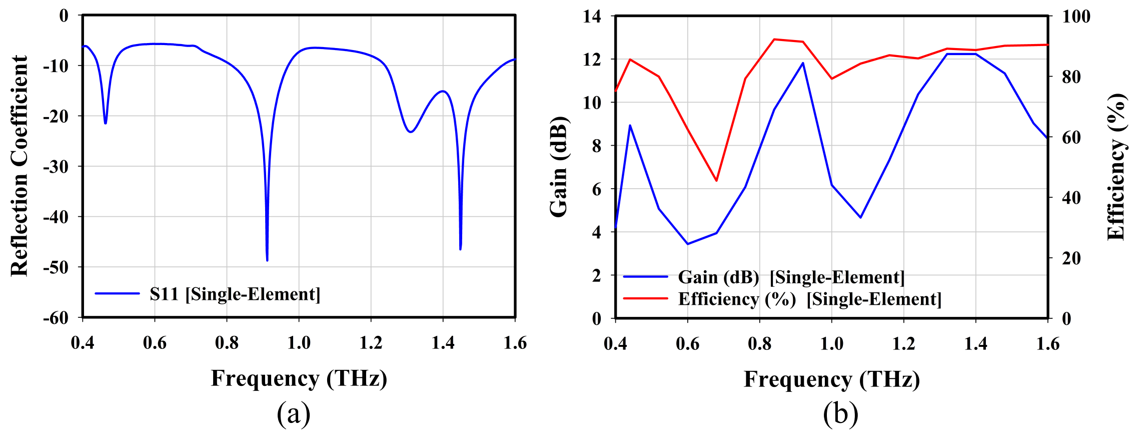

Figure 3. Simulated; (a) reflection coefficient and (b) gain and efficiency of the single-element antenna

2.2. Multiple-input multiple-output antenna

2.2.1. Reflection coefficient, gain and efficiency of proposed multiple-input multiple-output antenna

Figure 4(a) shows the reflection and transmission coefficients of the MIMO antenna at different frequencies. The figure shows four distinct resonance frequencies at 0.46 THz, 0.9 THz, 1.31 THz, and 1.44 THz with return losses of -27.64 dB, -53.18 dB, -37.6 dB, and -39.68 dB at these specific resonance frequencies. The bandwidths cover frequency ranges: 0.44-0.49 THz, 0.81-0.98 THz, and 1.25-1.59 THz, with bandwidths of 0.05 THz, 0.17 THz, and 0.34 THz, respectively. The MIMO antenna demonstrates a minimum isolation of -26 dB, as indicated by the transmission coefficient (S21). This high level of isolation indicates a lack of correlation between the antenna elements, ensuring the efficient and autonomous functioning of the numerous antenna elements in the MIMO system.

The MIMO antenna demonstrates significant performance in terms of gain and efficiency across its operational frequencies, as shown in Figure 4(b). The maximum simulated gain levels are 8.52 dB, 11.54 dB, and 13.25 dB. The MIMO antenna exhibits significant efficiency at its resonant frequencies. The maximum efficiencies are 88.32%, 92.02%, and 89.89%.

2.2.2. Envelope correlation coefficient and diversity gain

Figure 5(a) shows the ECC and Figure 5(b) DG of the proposed MIMO antenna. The optimal value of ECC for a statistically unaffected MIMO antenna is zero. However, it is recommended to set it below 0.5 for practical purposes [16]. The antenna's ECC is 0.003, indicating a shallow level of correlation between its two antenna elements.

$$ECC = \frac{\left|\int_{4\pi}\left[E_1(\theta,\varphi) * E_2(\theta,\varphi)\right] d\Omega\right|^2}{\int_{4\pi}\left|E_1(\theta,\varphi)\right|^2 d\Omega \int_{4\pi}\left|E_2(\theta,\varphi)\right|^2 d\Omega} \tag{1}$$

The MIMO antenna's DG is quantified as 9.98. The high DG value signifies that the antenna system offers substantial signal quality and reliability enhancements due to the diversity impact [17]. The DG, which is close to its maximum value, illustrates the antenna's capacity to retain high performance even in multipath situations, where signal reflections can impact the quality of communication [18].

$$DG = 10\sqrt{1 - ECC^2} \tag{2}$$

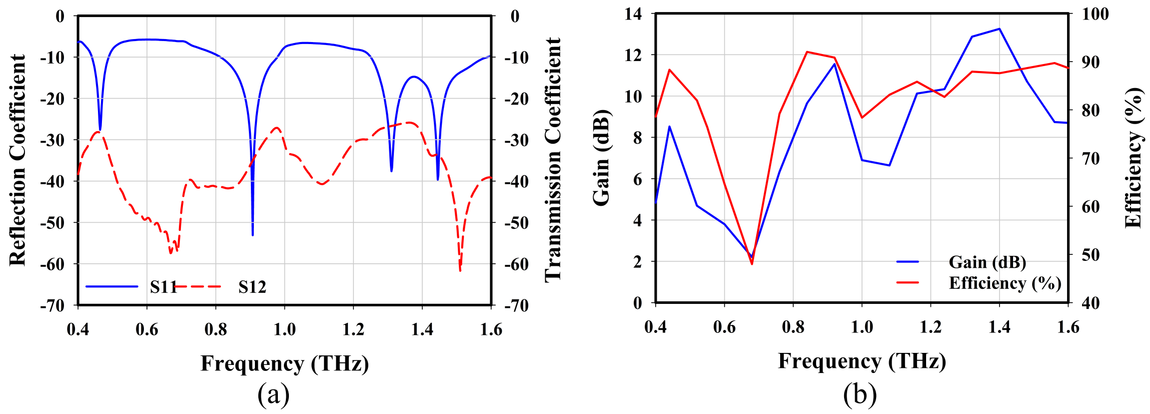

Figure 4. Simulated; (a) reflection coefficient, transmission coefficient and (b) gain and efficiency of the proposed MIMO antenna

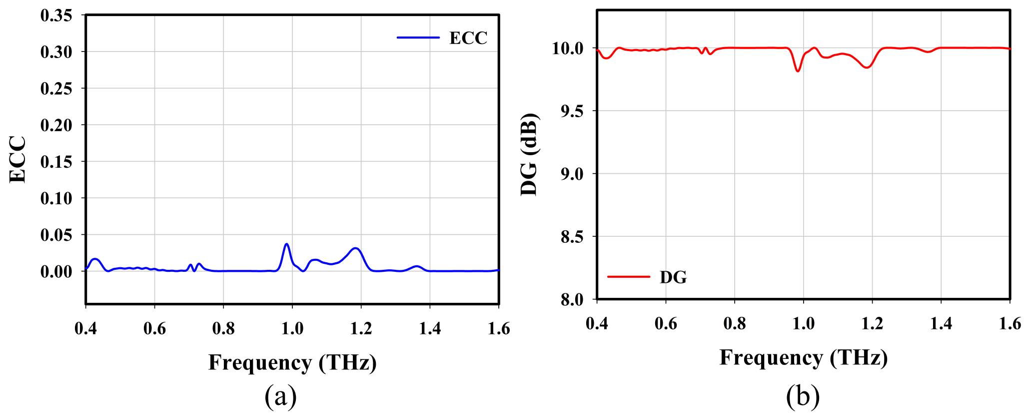

Figure 5. Simulated; (a) ECC and (b) DG of the proposed antenna

2.2.3. Radiation pattern of the proposed multiple-input multiple-output antenna

Figure 6 displays a polar plot illustrating the far-field E-field radiation pattern of an antenna, which is in operation at a frequency of 1 THz. The plot presents the magnitude of the electric field (in dBV/m) with respect to the angle (in degrees), covering a range from 0 to 360 degrees [19]. The data is specifically showcased for two planes, Phi=0 degrees and Phi=180 degrees [20]. The red line represents the broadband far-field radiation pattern. The key performance parameters of the antenna are detailed, including a main lobe magnitude of 12.8 dBV/m and a main lobe direction at 0.0 degrees. Furthermore, the plot indicates an angular width of 45.3 degrees, signifying the beamwidth at which the power diminishes to half its peak value (3 dB). Additionally, the side lobe level is highlighted at -5.9 dB, indicating secondary radiation lobes with lower intensity in comparison to the main lobe. This polar plot is an indispensable tool for visualizing the antenna's directional radiation characteristics, providing insights into the distribution and strength of the emitted signal across various angles.

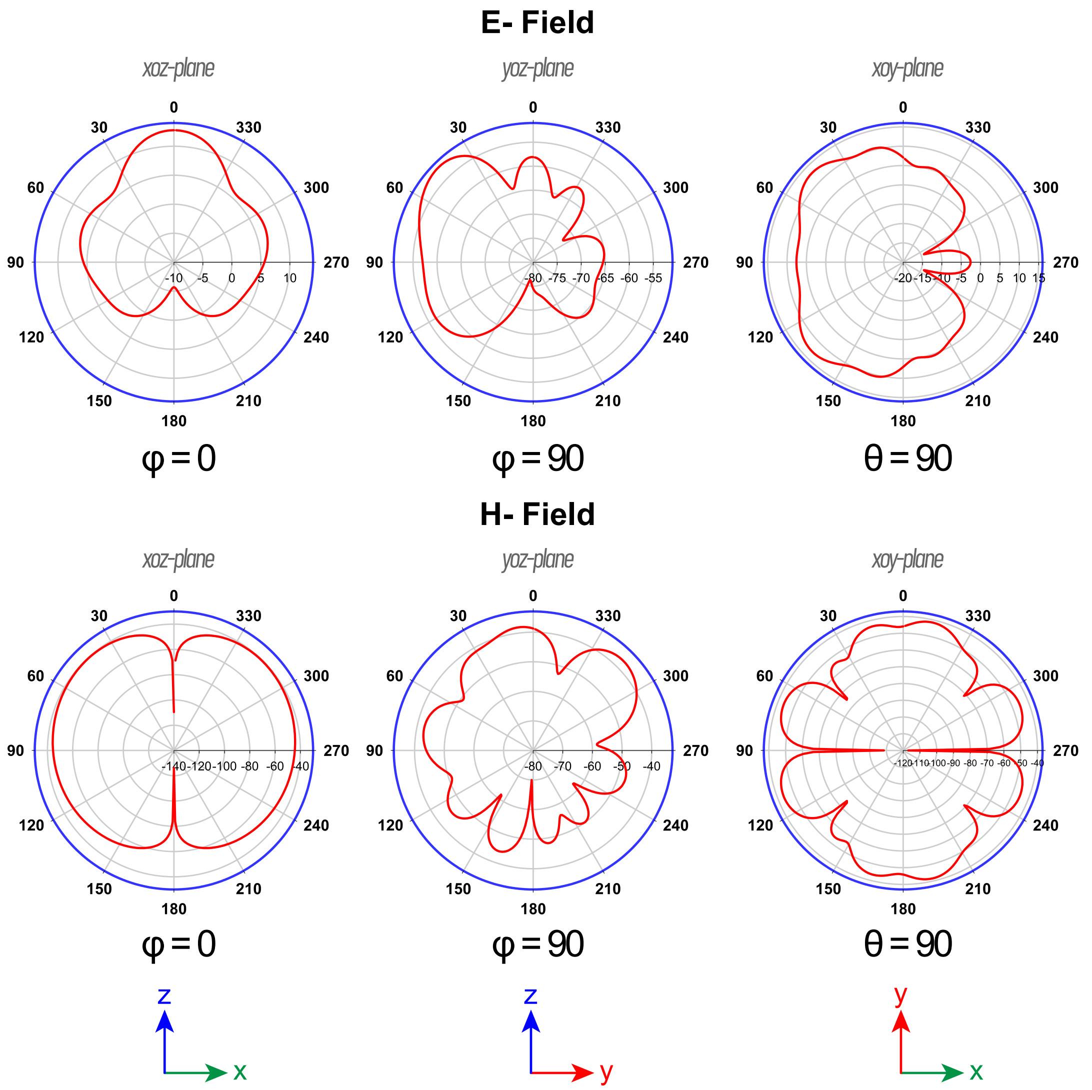

Figure 6. Radiation pattern of our proposed antenna

3. RLC EQUIVALENT CIRCUIT

An RLC equivalent circuit can represent an antenna and its impedance characteristics at different resonance frequencies [21]. A simplified model of an antenna, known as an RLC equivalent circuit, employs resistors (R), inductors (L), and capacitors (C) to replicate the impedance properties of the antenna across various frequencies [22]. A four-resonance antenna can be represented by an RLC equivalent circuit, where each resonance is defined by a unique combination of resistor (R), inductor (L), and capacitor (C) components [23]. The components (R1, L1, C1), (R2, L2, C2), (R3, L3, C3), and (R4, L4, C4) represent the resonance frequencies of the antenna, at which the impedance is solely resistive. The R, L, and C values for each resonance frequency are determined by utilizing CST to match the antenna's impedance data to the RLC model. The analogous circuit is subsequently created and simulated using advanced design system (ADS) to validate the antenna's performance at the selected resonance frequencies [24]. The ADS simulation entails configuring a frequency sweep and doing an S-parameter analysis to verify that the impedance characteristics align with the anticipated resonance frequencies [25]. This process confirms the precision of the RLC model in accurately portraying the antenna's performance. Figure 7 shows the RLC equivalent circuit of our proposed MIMO antenna.

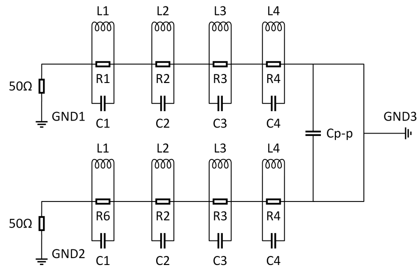

Figure 7. Design steps of single-element antenna.

4. CONCLUSION

The THz MIMO antenna's design employs copper for both the patch and ground plane, while utilizing a polyimide substrate. This design has been proven to be effective for operating within the 0.4 THz to 1.6 THz frequency range. The antenna exhibits resonant frequencies at 0.46 THz, 0.9 THz, and 1.31 THz, with corresponding bandwidths of 0.005 THz, 0.17 THz, and 0.34 THz. Notably, it achieves gains of 8.52 dB, 11.54 dB, and 13.25 dB, with high-efficiency levels of 88.32%, 92.02%, and 89.89% at these frequencies. Furthermore, the antenna demonstrates impressive isolation performance at 26 dB, coupled with a low ECC of 0.003 and a high DG of 9.98, which emphasizes its efficacy in MIMO systems. These findings validate the antenna's potential for integration into advanced THz communication systems, providing support for enhanced data transmission and reception capabilities. Additionally, the use of copper and polyimide materials ensures the antenna's reliability and performance stability, making it a promising solution for future wireless communication technologies.

ACKNOWLEDGMENTS

The author expresses gratitude to the Faculty of Graduate Studies and Department of Electrical and Electronic Engineering of Daffodil International University, Bangladesh, for their cooperation.

FUNDING INFORMATION

This research was funded by Daffodil International University, Dhaka, Bangladesh. No specific grant number is associated with this funding.

AUTHOR CONTRIBUTIONS STATEMENT

This journal uses the Contributor Roles Taxonomy (CRediT) to recognize individual author contributions, reduce authorship disputes, and facilitate collaboration.

Name of Author	C	M	So	Va	Fo	I	R	D	O	E	Vi	Su	P	Fu
Redwan Al Mahmud Bin Asad Ananta	✓		✓		✓				✓		✓			✓
Md. Sharif Ahammed		✓	✓	✓					✓					
Md. Ashraful Haque					✓					✓	✓	✓		
Narinderjit Singh Sawaran Singh		✓								✓				✓
Kamal Hossain Nahin		✓					✓	✓		✓				
Jamal Hossain Nirob						✓		✓		✓				
Md. Kawsar Ahmed						✓	✓			✓				
Liton Chandra Paul				✓	✓					✓			✓	

C : **C**onceptualization
M : **M**ethodology
So : **So**ftware
Va : **Va**lidation
Fo : **Fo**rmal Analysis
I : **I**nvestigation
R : **R**esources
D : **D**ata Curation
O : Writing - **O**riginal Draft
E : Writing - Review & **E**diting
Vi : **Vi**sualization
Su : **Su**pervision
P : **P**roject Administration
Fu : **Fu**nding Acquisition

CONFLICT OF INTEREST STATEMENT

The authors have no conflicts of interest to declare.

DATA AVAILABILITY

The data that support the findings of this study are available from the corresponding author (N.S.S.S) upon reasonable request.

REFERENCES

[1] H.-J. Song and T. Nagatsuma, "Present and Future of Terahertz Communications," in *IEEE Transactions on Terahertz Science and Technology*, vol. 1, no. 1, pp. 256–263, Sep. 2011, doi: 10.1109/TTHZ.2011.2159552.

[2] K. Rikkinen, P. Kyosti, M. E. Leinonen, M. Berg, and A. Parssinen, "THz Radio Communication: Link Budget Analysis toward 6G," in *IEEE Communications Magazine*, vol. 58, no. 11, pp. 22–27, Nov. 2020, doi: 10.1109/MCOM.001.2000310.

[3] R. Piesiewicz *et al*., "Short-Range Ultra-Broadband Terahertz Communications: Concepts and Perspectives," in *IEEE Antennas and Propagation Magazine*, vol. 49, no. 6, pp. 24–39, Dec. 2007, doi: 10.1109/MAP.2007.4455844.

[4] H. Vettikalladi, W. T. Sethi, A. F. B. Abas, W. Ko, M. A. Alkanhal, and M. Himdi, "Sub-THz Antenna for High-Speed Wireless Communication Systems," *International Journal of Antennas and Propagation*, vol. 2019, pp. 1–9, Mar. 2019, doi: 10.1155/2019/9573647.

[5] M. E. Benlakehal, A. Hocini, D. Khedrouche, M. N. E. Temmar, and T. A. Denidni, "Design and analysis of MIMO system for THz communication using terahertz patch antenna array based on photonic crystals with graphene," *Optical and Quantum Electronics*, vol. 54, no. 11, p. 693, Nov. 2022, doi: 10.1007/s11082-022-04081-0.

[6] K. M. Luk et al., "A microfabricated low-profile wideband antenna array for terahertz communications," *Scientific Reports*, vol. 7, no. 1, p. 1268, Apr. 2017, doi: 10.1038/s41598-017-01276-4.

[7] Z. Xu, X. Dong, and J. Bornemann, "Design of a Reconfigurable MIMO System for THz Communications Based on Graphene Antennas," *IEEE Transactions on Terahertz Science and Technology*, vol. 4, no. 5, pp. 609–617, Sep. 2014, doi: 10.1109/TTHZ.2014.2331496.

[8] S. A. Khaleel, E. K. I. Hamad, N. O. Parchin, and M. B. Saleh, "MTM-Inspired Graphene-Based THz MIMO Antenna Configurations Using Characteristic Mode Analysis for 6G/IoT Applications," *Electronics*, vol. 11, no. 14, p. 2152, Jul. 2022, doi: 10.3390/electronics11142152.

[9] K. Vasu Babu, S. Das, G. Varshney, G. N. J. Sree, and B. T. P. Madhav, "A micro-scaled graphene-based tree-shaped wideband printed MIMO antenna for terahertz applications," *Journal of Computational Electronics*, vol. 21, no. 1, pp. 289–303, Feb. 2022, doi: 10.1007/s10825-021-01831-3.

[10] B. Zhang, J. M. Jornet, I. F. Akyildiz, and Z. P. Wu, "Mutual coupling reduction for ultra-dense multi-band plasmonic nano-antenna arrays using graphene-based frequency selective surface," *IEEE Access*, vol. 7, pp. 33214-33225, 2019, doi: 10.1109/ACCESS.2019.2903493.

[11] P. Das, "Beam-steering of THz MIMO antenna using graphene-based intelligent reflective surface," *Optical and Quantum Electronics*, vol. 55, no. 8, p. 711, Aug. 2023, doi: 10.1007/s11082-023-04996-2.

[12] N. K. Maurya, S. Kumari, P. Pareek, and L. Singh, "Graphene-based frequency agile isolation enhancement mechanism for MIMO antenna in terahertz regime," *Nano Communication Networks*, vol. 35, p. 100436, Mar. 2023, doi: 10.1016/j.nancom.2023.100436.

[13] C. Vamsi, A. K. Dwivedi, G. Bharti, V. R. Verma, and A. Sharma, "Efficient graphene-based circularly polarized MIMO antenna for THz applications," *Applied Optics*, vol. 61, no. 28, p. 8155, Oct. 2022, doi: 10.1364/AO.462531.

[14] M. Alibakhshikenari *et al*., "High-Gain On-Chip Antenna Design on Silicon Layer With Aperture Excitation for Terahertz Applications," in *IEEE Antennas and Wireless Propagation Letters*, vol. 19, no. 9, pp. 1576–1580, Sep. 2020, doi: 10.1109/LAWP.2020.3010865.

[15] Md. A. Haque *et al*., "Machine learning-based technique for gain prediction of mm-wave miniaturized 5G MIMO slotted antenna array with high isolation characteristics," *Scientific Reports*, vol. 15, no. 1, p. 276, Jan. 2025, doi: 10.1038/s41598-024-84182-w.

[16] Md. A. Haque *et al*., "Machine learning based compact MIMO antenna array for 38 GHz millimeter wave application with robust isolation and high efficiency performance," *Results in Engineering*, vol. 25, p. 104006, Mar. 2025, doi: 10.1016/j.rineng.2025.104006.

[17] M. Salehi and M. Manteghi, "Transient Characteristics of Small Antennas," *IEEE Transactions on Antennas and Propagation*, vol. 62, no. 5, pp. 2418–2429, May 2014, doi: 10.1109/TAP.2014.2307353.

[18] F. Ez-Zaki *et al*., "Circuit Modelling of Broadband Antenna Using Vector Fitting and Foster Form Approaches for IoT Applications," *Electronics*, vol. 11, no. 22, p. 3724, Nov. 2022, doi: 10.3390/electronics11223724.

[19] S. S. Al-Bawri *et al*., "Machine learning technique based highly efficient slotted 4-port MIMO antenna using decoupling structure for sub-THz and THz 6G band applications," *Optical and Quantum Electronics*, vol. 56, no. 10, p. 1611, Sep. 2024, doi: 10.1007/s11082-024-07249-y.

[20] M. A. Haque *et al*., "Performance improvement of THz MIMO antenna with graphene and prediction bandwidth through machine learning analysis for 6G application," *Results in Engineering*, vol. 24, p. 103216, Dec. 2024, doi: 10.1016/j.rineng.2024.103216.

[21] K. H. Nahin *et al*., "Performance prediction and optimization of a high-efficiency tessellated diamond fractal MIMO antenna for terahertz 6G communication using machine learning approaches," *Scientific Reports*, vol. 15, no. 1, p. 4215, Feb. 2025, doi: 10.1038/s41598-025-88174-2.

[22] S. Das, D. Mitra, and S. R. Bhadra Chaudhuri, "Fractal loaded planar Super Wide Band four element MIMO antenna for THz applications," *Nano Communication Networks*, vol. 30, p. 100374, Dec. 2021, doi: 10.1016/j.nancom.2021.100374.

[23] N. S. Asaad, A. M. Saleh, and M. A. Alzubaidy, "Analyzing Performance of THz Band Graphene-Based MIMO Antenna for 6G Applications," *Journal of Telecommunications and Information Technology*, Jul. 2024, doi: 10.26636/jtit.2024.3.1518.

[24] M. Esfandiyari, S. Jarchi, and M. Ghaffari-Miab, "Channel capacity enhancement by adjustable graphene-based MIMO antenna in THz band," *Optical and Quantum Electronics*, vol. 51, no. 5, p. 137, May 2019, doi: 10.1007/s11082-019-1856-2.
[25] K. V. Babu, S. Das, G. N. J. Sree, B. T. P. Madhav, S. K. K. Patel, and J. Parmar, "Design and optimization of micro-sized wideband fractal MIMO antenna based on characteristic analysis of graphene for terahertz applications," *Optical and Quantum Electronics,*, vol. 54, no. 5, p. 281, May 2022, doi: 10.1007/s11082-022-03671-2.

BIOGRAPHIES OF AUTHORS

Redwan Al Mahmud Bin Asad Ananta has accomplished his undergraduate studies in the field of Electrical and Electronics at Daffodil International University. His research focus encompasses wireless communication, specifically antenna arrays, MIMO antennas, metamaterials and metasurfaces for mm-Wave, subTerahertz, and Terahertz band applications. He can be contacted at email: redwan33-1145@diu.edu.bd.

Md. Sharif Ahammed is a student of Daffodil International University and pursuing a B.Sc. in the Department of Electrical and Electronics. He passed from Government Bangabandhu college with a higher secondary. Microstrip patch antenna, terahertz antenna, and 5G application, biomedical applications are some of his research interests. He can be contacted at email: sharif33-1152@diu.edu.bd.

Md. Ashraful Haque is doing Ph.D. at the Department of Electrical and Electronic Engineering, Universiti Teknologi PETRONAS, Malaysia, He got his B.Sc. in Electronics and Electronic Engineering (EEE) from Bangladesh's Rajshahi University of Engineering and Technology (RUET) and his M.Sc. in the same field from Bangladesh's Islamic University of Technology (IUT). He is currently on leave from Daffodil International University (DIU) in Bangladesh. His research interest includes microstrip patch antenna, sub 6 5G application, and supervised regression model machine learning on antenna design. He can be contacted at email: limon.ashraf@gmail.com.

Narinderjit Singh Sawaran Singh is a Associate Professor in INTI International University, Malaysia. He graduated from the Universiti Teknologi PETRONAS (UTP) in 2016 with Ph.D. in Electrical and Electronic Engineering specialized in Probabilistic methods for fault tolerant computing. Currently, he is appointed as the research cluster head for computational mathematics, technology and optimization which focuses on the areas like pattern recognition and symbolic computations, game theory, mathematical artificial intelligence, parallel computing, expert systems and artificial intelligence, quality software, information technology, exploratory data analysis, optimization algorithms, stochastic methods, data modelling, and computational intelligence-swarm intelligence. He can be contacted at email: narinderjits.sawaran@newinti.edu.my.

Kamal Hossain Nahin currently pursuing a degree in Electrical and Electronic Engineering at Daffodil International University. His educational journey commenced at Ishwardi Govt College for Higher Secondary Certificate (HSC) and earlier at Maniknagar High School for Secondary School Certificate (SSC). Embarking on a journey as a budding researcher in the communication field, He is passionately immersed in exploring the realms of wireless communication. His focus lies in delving into the intricacies of wireless communication, particularly exploring microstrip patch antennas, terahertz antennas, and their potential applications in the future realms of 5G and 6G technologies. He can be contacted at email: kamal33-1242@diu.edu.bd.

Jamal Hossain Nirob is a student in the Department of Electrical and Electronic Engineering (EEE) at Daffodil International University. His educational journey began at Maniknagar High School, where he successfully completed his Secondary School Certificate (SSC). Following that, he pursued higher studies at Ishwardi Government College, obtaining his Higher Secondary Certificate (HSC). With a strong enthusiasm for expanding communication technology, Jamal has focused his research on wireless communication, specifically on microstrip patch antennas, terahertz antennas, and applications of 5G and 6G. He can be contacted at email: jamal33-1243@diu.edu.bd.

Md. Kawsar Ahmed is currently pursuing his studies in the field of Electrical and Electronic Engineering at Daffodil International University. He successfully finished his Higher Secondary education at Agricultural University College, Mymensingh. He is presently employed as a student associate at Daffodil International University (DIU) in Bangladesh. The areas of his research focus encompassed microstrip patch antennas, terahertz antennas, and applications related to 4G and 5G technologies. He can be contacted at email: kawsar33-1241@diu.edu.bd.

Liton Chandra Paul is successfully finished his master's degree in Electrical and Electronic Engineering (EEE) and bachelor's degree in Electronics and Telecommunication Engineering (ETE) in 2015 and 2012, respectively. Throughout his time as a student, he has made generous contributions to numerous nonprofit social welfare organizations. His research interests are RFIC, bioelectromagnetic, microwave technology, antennas, phased arrays, mmWave, metamaterials, metasurfaces, and wireless sensors. He can be contacted at email: litonpaulete@gmail.com.